Estuarine, Coastal and Shelf Science 219 (2019) 341–353

Contents lists available at ScienceDirect

Estuarine, Coastal and Shelf Science

journal homepage: www.elsevier.com/locate/ecss

Near shore distributions of phytoplankton and bacteria in relation to submarine groundwater discharge-fed fishponds, Kona coast, Hawai'i, USA

Jason E. Adolf[a,*], John Burns[a], Judy K. Walker[a], Sydney Gamiao[b]

[a] University of Hawaii Hilo, Marine Science Department and TCBES Graduate Program, USA
[b] University of Hawaii Hilo College of Agriculture, USA

ARTICLE INFO

Keywords:
Hawaii
Hawaiian fishponds
Phytoplankton
Submarine groundwater discharge

ABSTRACT

Phytoplankton are important components of coastal marine ecosystems that are strongly influenced by freshwater inputs from land, including submarine groundwater discharge (SGD). Although SGD generates sharp onshore – offshore gradients in physical and chemical conditions at several locations around Hawaii Island little is known about the biotic responses of water column microbes to these conditions. We studied the distributions of phytoplankton and bacteria at two contrasting sites with SGD-fed fishponds, Kiholo and Kaloko Bay, including the full range of salinity extending from the fishponds to the coastal ocean. We addressed the hypotheses that (1) SGD-fed fishponds support a higher biomass and different composition of phytoplankton than the adjacent ocean, and (2) phytoplankton biomass and composition are related to SGD-driven salinity gradients in the coastal ocean. Phytoplankton biomass in fishponds was elevated (10–100-fold) and accompanied by higher average cell size pico- and nano-phytoplankton (2–6 μm) relative to sites outside the fishpond. General additive models (GAMs) showed elevated biomass and average cell size at mid-range salinities and declining biomass at salinity < 20 outside the fishponds. Multivariate RDA showed significant, site-specific relationships between surface phytoplankton biomass (Chl *a*), cell counts, and environmental parameters. Analysis of surface vs. deep samples from outside the fishponds showed elevated phytoplankton biomass at the surface, except in Kiholo lagoon where phytoplankton was elevated beneath the SGD-driven pycnocline. This study shows structuring of coastal phytoplankton through SGD inputs and suggest that changes in SGD due to coastal development or climate change can impact coastal marine ecosystems through effects on phytoplankton communities.

1. Introduction

Submarine groundwater discharge (SGD), generally defined as fresh groundwater or a mix of groundwater and recirculated seawater discharging to the coastal ocean, is an important source of new nutrients to phytoplankton and other organisms in coastal ecosystems (Valiela et al., 1990; Slomp and Van Capellan; 2004; Paerl, 1997; Paytan et al., 2006; Burnett et al., 2006; Kim et al., 2008). The contribution of SGD-derived nutrients can rival or surpass that supplied by surface waters (Johannes, 1980; Slomp and Van Capellan, 2004; Garrison et al., 2003; Kim et al., 2005), either through elevated nutrient concentrations compared to surface runoff, or via persistent groundwater flows in environments where surface runoff is not common (Shellenbarger et al., 2006; Knee et al., 2008). Volcanic high islands can have very high rates of coastal SGD and nutrient delivery because of upland orographic rainfall and the high permeability of basalt substrate (Oki et al., 1999; Kim and Lee, 2003; Tribble, 2008; Kim et al., 2011; Moosdorf et al., 2014).

The oligotrophic waters of the North Pacific Tropical Gyre (NPTG) surrounding the main Hawaiian Islands (MHI) are met in many places by nutrient-rich plumes of SGD that generate sharp horizontal and vertical gradients of physical and chemical properties (Garrison et al., 2003; Johnson et al., 2008; Street et al., 2008; Knee et al., 2010) in the coastal ocean. Waters entering the ocean via the subterranean estuary, defined by Moore (1999) as 'a coastal aquifer where groundwater derived from land measurably dilutes seawater that has invaded the aquifer through a free connection to the sea', can have lower salinity and temperature than sea water, and elevated nitrate, silica and phosphate that in some cases reflects waste water contamination (Knee et al., 2010). Thermal infrared imagery has been used to document the frequency and size (generally within 1 km of the shoreline) of SGD plumes along the Hawaiian coastline because of the distinct 5–7 °C cooler temperatures associated with groundwater relative to the ocean (Johnson et al., 2008). Coastal plumes of SGD are buoyant, resulting in

* Corresponding author. Monmouth University, Biology Department, 400 Cedar Ave., West Long Branch, NJ 07764. USA.
E-mail address: jadolf@monmouth.edu (J.E. Adolf).

https://doi.org/10.1016/j.ecss.2019.01.021
Received 2 March 2018; Received in revised form 24 January 2019; Accepted 27 January 2019
Available online 05 February 2019
0272-7714/

varying degrees of stratification depending on the strength and proximity of the SGD source (Bienfang, 1980; Dollar and Atkinson, 1992; Johnson et al., 2008). Submarine groundwater discharge dominates as a freshwater source to the ocean on the arid, leeward side of Hawaii Island, including the Kona coast.

Traditional Hawaiian fishponds are often fed by SGD, including the 400 yr old 11-acre Kaloko Fishpond within Kaloko-Honokohau National Historic Park (Kikuchi, 1976; Bond and Gmirkin, 2003). Native Hawaiians were intuitive engineers who constructed coastal fishponds, or *loko,* by strategically stacking porous lava rocks to form a wall delineating an inundated space connected to the ocean by one or more small sluice gates called a *makaha*. The *makaha* allowed for a limited exchange of water between the fishpond and the surrounding ocean resulting in longer residence time and brackish water conditions that favored the food species raised there (Kikuchi, 1976). The retention of water behind semi porous walls, along with the inputs of nutrient-rich groundwater, makes these ponds sensitive to eutrophication or other contamination from polluted groundwater (Valiela et al., 1990; Nixon et al., 2007; Lapointe et al., 1990).

Submarine groundwater discharge has been shown to influence phytoplankton and other biological communities through various direct and indirect mechanisms. Elevated phytoplankton biomass has been attributed to nutrients supplied by SGD in a Mediterranean embayment (Rodellas et al., 2014), as well as SGD-influenced sites along the north coast of the Yucatan peninsula (Herrera-Silveira, 1998; Morales-Ojeda et al., 2010), although Medina-Gomez and Herrera-Silvera (2006) described suppression of phytoplankton growth by reduced residence time due to river and groundwater flow despite elevated inorganic nutrient abundance. Elevated Chl *a* has been documented in traditional Hawaiian fishponds fed by SGD (Bienfang, 2007), as well as other tropical environments influenced by SGD (Laws et al., 2004; Marsh, 1977). Surf zone phytoplankton production on sandy shores has been linked to SGD (reviewed by Odebrecht et al., 2014). Effects of SGD on phytoplankton community composition were described by Alvarez-Gongora and Herrera-Silveira (2006), and Troccoli-Ghiaglia et al. (2010) in waters of the Yucatan Peninsula, and for phytoplankton over a fringing reef by Blanco et al. (2008). Harmful algal blooms (HAB) have been linked to SGD, including *Aureococcus* in Long Island Sound (Gobler and Sanudo-Wilhelmy, 2001) and *Cochlodinium polykrikoides* in the sea of Korea (Lee and Kim, 2007; Lee et al., 2010). Interestingly, in both of these cases the HAB species followed non-HAB blooms that transformed SGD-nutrients generating beneficial conditions for the HAB to occur. Bioassay experiments, where seawater is experimentally supplemented with local groundwater (Garces et al., 2011; Lecher et al., 2015; Chamberlain et al., 2014) show elevated phytoplankton biomass and accompanying changes in community composition. Submarine groundwater discharge was included among the potential mechanisms underlying the so-called 'Island Mass Effect' responsible for phytoplankton enhancements around a majority of Pacific island/atoll ecosystems (Gove et al., 2016).

Oligotrophic phytoplankton assemblages, such as those surrounding the Hawaiian Islands, are generally characterized by low Chl *a* biomass ($< 1\ mg\ m^{-3}$) and a predominance of small cells (picophytoplankton $< 2\ \mu m$) that are tightly coupled to grazers (Landry et al., 1984; Karl et al., 2002; Calbet and Landry, 2004; Calbet and Saiz, 2005; Brown et al., 2008). Accumulations of Chl *a* biomass in such environments are often accompanied by a change in community composition including a shift to predominance by larger size classes of cells, which can impact the fate of phytoplankton in coastal ecosystems (Chisholm, 1992; Thingstad, 1997; Irwin et al., 2006; Goericke, 2011). Since phytoplankton are important primary producers in coral reef ecosystems (Wabnitz et al., 2010), and nutrient-enhanced phytoplankton productivity in tropical/subtropical systems can lead to detrimental impacts on coral reefs (Bell et al., 2014) such as increased abundance of bioeroders (i.e. *Acanthaster*), heterotrophic filter feeders that compete with corals, and macroalgal biomass (Fabricus, 2005), understanding phytoplankton-nutrient dynamics over coral reef ecosystems receiving anthropogenic nutrient inputs is essential.

The arid leeward side of Hawai'i Island is an ideal study area for investigation of fishpond - groundwater – phytoplankton linkages on Pacific high islands because of very low local rainfall and surface runoff, making salinity a good indicator of SGD (Knee et al., 2010), as well as the presence of numerous traditional Hawaiian fishponds along the coast. This study examined distributions of water quality parameters, phytoplankton and heterotrophic bacteria along the salinity gradient extending from traditional Hawaiian fishponds at two contrasting sites in West Hawai'i, Kaloko and Kiholo Bays, focusing on phytoplankton biomass and community composition. Hypotheses addressed included (1) fishponds would support a higher biomass and different composition of phytoplankton than the adjacent ocean, and (2) phytoplankton biomass and composition are related to SGD salinity gradients in the coastal ocean.

2. Methods

2.1. Site descriptions

Kiholo Bay and Kaloko-Honokohau National Historical Park lie on the arid leeward coast of Hawaii Island (Fig. 1). These sites were chosen for their contrasts: while they share a predominance of SGD as a freshwater input and SGD-fed fishponds, they differ in some key watershed characteristics, including the size and configuration of their respective fishponds, as further detailed below. Annual rainfall at Kiholo Bay is 271.1 mm; average annual rainfall at Kaloko-Honokohau is 469.0 mm (Giambelluca et al., 2013), but groundwater dominates freshwater inputs to the ocean (Peterson et al., 2009). The Kiholo Bay watershed is relatively undeveloped, while the Kaloko-Honokohau watershed includes a county landfill, a wastewater treatment injection well, a golf course, and rapidly expanding residential and industrial areas (DeVerse, 2006; Knee et al., 2008). Further, the 11-acre fishpond at Kaloko differentiates this site from Kiholo which has a small fishpond. Both sites are documented areas of high SGD where fresh SGD can be observed as a buoyant plume of cooler, brackish water (Johnson; 2008; Street et al., 2008; Peterson et al., 2009; Knee et al., 2010). SGD input at Kiholo Bay is estimated to be 6300 m^3d^{-1} from a lagoon adjacent to the bay (using geochemical tracers) to 9200 m^3d^{-1} from a 110 m transect along the shore (using electrical resistivity methods) (Peterson et al., 2009; Dimova et al., 2012). There are no estimates encompassing the specific area of Kaloko-Honokohau sampled in this study, but various areas of the park were estimated to be 10–382 $m^3\ d^{-1}$ (Knee et al., 2010). Modeling of Kaloko-Honokohau estimated 6.48 Mgal d^{-1} of fresh SGD input in the park as a whole, or about 3 Mgal d^{-1} per mile of coastline (Oki et al., 1999). This is equivalent to approximately 11,300 m^3d^{-1} *per mile* of coastline, much less than the amount of fresh SGD estimated at Kiholo Bay.

2.2. Water sampling

Kaloko was sampled June and July 2010; March, June and July 2011; and March 2012. Kiholo was sampled September 2010; March, June and August 2011; and March 2012. Every field trip included at least one offshore station with full strength seawater salinity and outside the direct influence of the SGD plume. Stations were sampled in the morning near low tide to minimize water column mixing and maximize the likelihood of observing the physical effects of the SGD plume (Burnett et al., 2003; Dimova, 2012).

Water samples (500 mL) were collected from the surface (Fig. 1, all stations) and bottom of the water column concurrently with the depth profiles (select stations) using a Wildco Beta Water Sampler. At deep offshore stations, samples were collected in excess of 20 m depth rather than at the actual bottom. Salinity of water samples was measured using a multiparameter meter (YSI Model 85). Samples were processed for nutrient and Chl *a* concentration, and 15 mL subsamples were

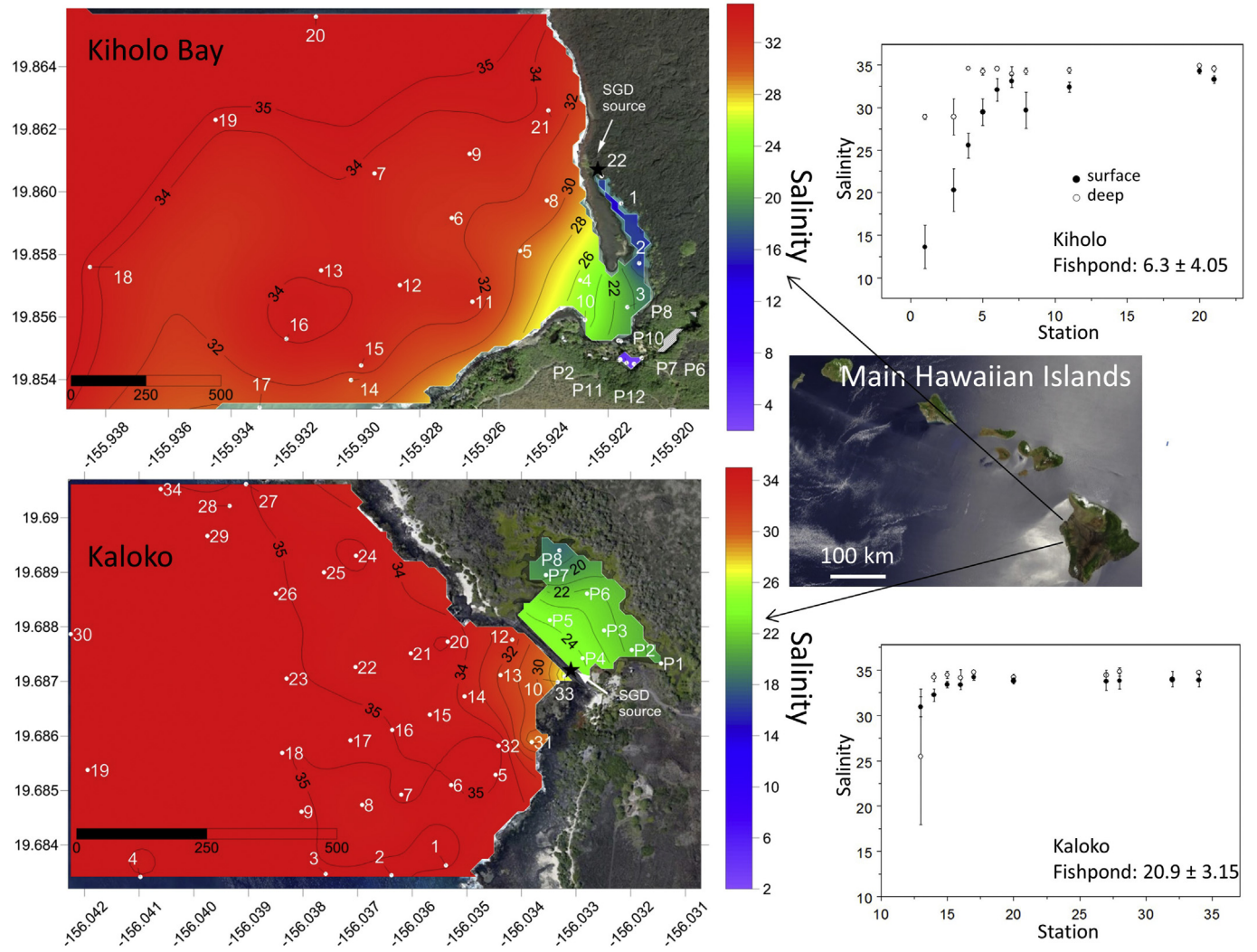

Fig. 1. Site maps showing average salinity (black isohalines/fill) and stations (white labels). Site map scale is meters. Vertical profile stations were Kaloko Sta 13, 14, 15, 17, 19, 20, & 21; Kiholo sta 1, 3, 4, 5, 6, 7, 8, 11, 20, &21). Surface and deep water salinity (± se) is shown for these station to the right of each map.

preserved with a final concentration of 0.5% gluteraldehyde, allowed to fix on ice for 30 min before being frozen on dry ice until transfer to a −80 °C freezer for storage for flow cytometric analysis of phytoplankton and bacteria.

Vertical profile sampling stations were designated at Kiholo and Kaloko (Fig. 1). Salinity and temperature were measured *in situ* from the surface to within a meter of the substrate using a multiparameter water quality sonde (Yellow Springs Instruments 6600 V2-4, 1 Hz sampling frequency). Data were binned into 0.2 m intervals between z = 0 m and z = 3 m; 0.5 m bins between 3 m and 6 m; 2 m bins for depths greater than 6 m. Additional surface samples were taken in a grid pattern at each site (Fig. 1).

2.3. Nutrient and Chl a sample analyses

Water samples were filtered through muffled (6 h at 500 °C) Whatman GF/F filters. Samples were stored frozen until analysis. Samples were analyzed for NO_3^- + NO_2^- (referred to hereafter as simply NO_3^-), PO_4^{3-}, and H_4SiO_4, with concentrations of NO_3^- + NO_2^- (USEPA 353.4), PO_4^{3-} (USEPA 365.5), and H_4SiO_4 (USEPA 366) determined using a Technicon Pulse II AutoAnalyzer having instrument method detection limits of 0.1 µm for NO_3^-, 0.10 µm for PO_4^{3-}, and 1.0 µm for H_4SiO_4. The filter was saved for chl *a* analysis, with filters flash frozen in foil on dry ice and transferred to a −80 °C freezer until analysis. Chl *a* analysis was performed using a modified U.S. EPA method 445.0 on a Turner Designs Model 10AU fluorometer.

2.4. Flow cytometric data acquisition

Data were acquired on an Accuri C6 flow cytometer equipped with two lasers (488 nm and 640 nm) and standard Optical filters FL1 530/30 nm, FL2 585/40 nm, FL3 > 670 nm, and FL4 675/25 nm; C-Sampler software was used with the C-Sampler automatic sampler and 48 well plates. Controls on the plate included 0.2 µm filtered water in the first and every 8th well. Absolute counting accuracy was verified and calibrated by Countbrite beads (Invitrogen). Spherotech Rainbow Calibration Particles, 8-Peak (Accuri QA100, for voltage settings on FL1, 2 and 3 and FSC, SSC) are run routinely to verify instrument specifications according to the manufacturer.

Data acquisition was triggered on FL-1 using an empirically determined threshold of 600, which minimized electronic noise while maximizing the sensitivity of the C6 for phytoplankton. Each well was sampled for 2 min on medium speed (34 µL min^{-1}). The 48 well plate was agitated once, and the sample injection port washed once, before each sample was run. Heterotrophic bacteria were enumerated after staining samples with SYTO BC (Invitrogen) at a rate of 1 µL per mL sample. Plates were stained for 10 min at room temperature in

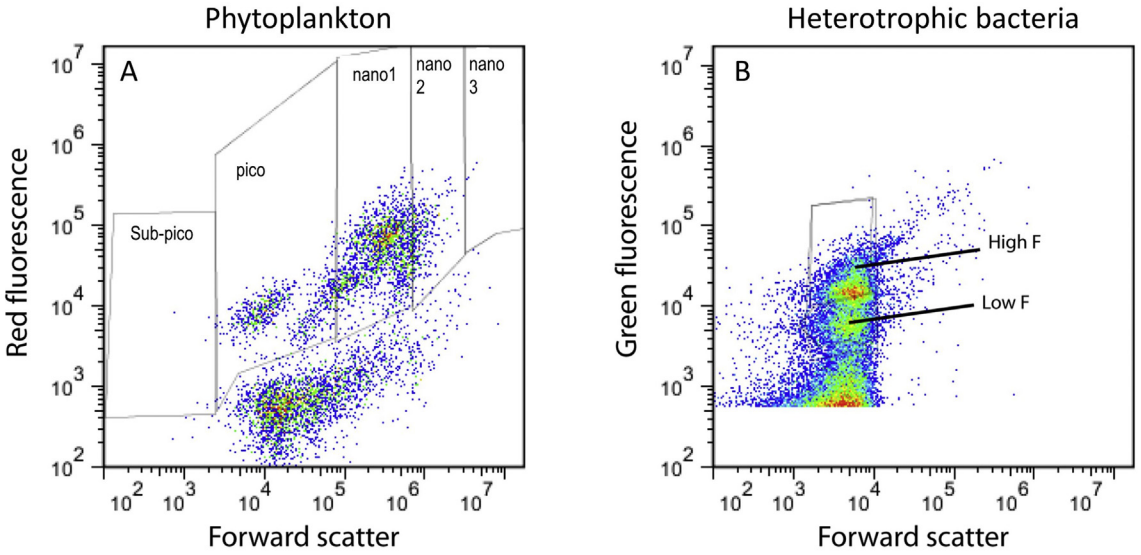

Fig. 2. Example flow cytometric density biplots used for (A) phytoplankton and (B) heterotrophic bacteria stained with SYTO BC. 'Forward scatter' is the FSC-H channel on the Accuri-C6 while 'Red fluorescence' and 'Green fluorescence' are the FL3-H and FL1-H channels, respectively. Phytoplankton regions correspond to picophytoplankton ('pico') and three sub-categories of nanophytoplankton based on size. The 'sub-pico' region was not used in the analysis.

darkness. Each well was sampled for 20 s, yielding approximately 11 μL sampled volume.

2.5. Flow cytometry data analysis

Four size categories of phytoplankton were quantified in empirically-determined regions on a biplot of forward angle scatter (FSC—H) vs. red fluorescence (FL3-H) using FlowJo 7.6 software (Fig. 2A). The FlowJo analysis template file is available (jadolf@monmouth.edu) to allow replication of the particle analyses presented here. This method allowed objective analysis across all samples collected throughout the study, avoiding the need for subjective selection of populations on 100's of flow cytometry samples analyzed. Phytoplankton were distinguished from non-phytoplankton particles based on an empirically determined FL3-H threshold that increased as FSC-H increased, and distinguished by size based on four regions (PICO, NANO1, NANO 2, NANO 3) (Fig. 2A). The PICO region was monitored on both the red and orange fluorescence channels to confirm *Synechococcus* and reported as R.PICO and O.PICO, respectively. We found *Synechococcus* in all samples we analyzed, but our flow cytometric method did not enumerate *Prochlorococcus*. While *Prochlorococcus* is common in the NPTG, these phytoplankton are not significantly abundant in nearshore areas and coastal embayments around Hawaii (Cox et al., 2006). Equivalent spherical diameter (ESD), used as an indicator of phytoplankton cell size within each size region, was determined based on calibration of geometric mean FSC-H against latex beads of known diameter (0.5–15 μm; Invitrogen flow cytometry size standards), as well as cultured phytoplankton whose size was measured at the microscope (*Synechococcus* sp., *Cryptomonas* sp, *Amphidinium* sp.) (ESD (μm) = $0.0048(FSC-H)^{0.5296}$) $r^2 = 0.89$). For each sample, the geometric mean FSC-H, geometric mean FL3-H, and the events mL^{-1} was reported for each of the regions. Avg. ESD is the weighted average ESD across the four size regions, where fraction of total phytoplankton cell count for each region is used as the weighting parameter. Equivalent spherical volume mL^{-1} (ESV mL^{-1}), used as an indicator of phytoplankton biomass (biovolume, μm^3 mL^{-1}), was calculated by converting ESD to ESV (4/3 pi r^3), where r (radius) is calculated from the ESD, to yield the geometric mean biovolume $cell^{-1}$ in each region. ESV mL^{-1} is then calculated as the summation of the product of ESV and cells mL^{-1} across regions. A similar phytoplankton biovolume metric was used by Li et al. (1993). High fluorescence and low fluorescence bacteria were enumerated on a biplot of FL1-H (green fluorescence) vs. FSC-H. The measured FSC varied little (3.5%) for the bacterial populations we measured, so we used a constant cell biovolume (0.050 μm^3 $cell^{-1}$) calculated from our FSC – cell diameter calibration curve to estimate bacterial biovolume in the same units used for phytoplankton (μm^3 mL^{-1}).

2.6. Statistical analyses

Only a subset of surface stations at each site had paired bottom water samples (Fig. 1, KI 1–8,11, 20, 21; KA 13–17,19), so individual ANOVA were run to compare surface and bottom parameters at those stations, using only the paired surface/bottom samples, *eg.* only concurrently sampled surface/bottom parameters were used in these comparisons.

Phytoplankton parameters ESD, Chl *a,* ESV, and heterotrophic bacteria cell counts were modelled as a function of salinity using generalized additive models (GAM). A GAM is a flexible statistical model that allows for dealing with non-linear and non-monotonic relationships between the response and explanatory variables. Log-transformed values of Chl *a,* ESV, and heterotrophic bacteria were used to develop the GAMs. A model was fit for each response variable (ESD, log-Chl *a,* ESV, and heterotrophic bacteria) as a function of salinity at each site (Kiholo and Kaloko). GAMs were built using cubic regression splines as a standard smoothing approach with the 'mgcv' package in R. The GAMs determine if statistically significant non-linear relationships exist between salinity and the explanatory variables at both study sites. The analyses and results presented here were conducted using R statistical software version 3.5.1.

Redundancy analyses (RDA) were performed separately for Kiholo and Kaloko sites with all data combined (surface, deep, pond, ocean) in order to produce a large enough sample size for each site. Replicate samples for any given station taken at different times were averaged and all water quality parameters were standardized for these analyses. Redundancy analyses combined multiple linear regression with a principle component analysis (PCA) of the table of fitted values (Borcard et al., 2011). The RDA procedure is a constrained analysis; thus, the results show variation in the response variables (cell counts) that are associated with the water quality parameters. This method is useful for identifying how cell counts are affected by physical water quality parameters and provides a comprehensive approach for

Table 1
Geometric mean (± SE) by class for abundance (cells mL^{-1}), cell size (ESD, μm), and biovolume (ESV, μm^3 mL^{-1}). Sample size (*n*) for all calculations is 690, except for nano2 and nano3 ESD wherein samples with zero abundance were excluded, yielding n = 683 and 116, respectively.

Class	cells mL^{-1}	ESD (μm)	ESV mL^{-1}
Hbact	477253 ± 47119.8	0.5 ± 0.001	23653 ± 2054.7
rpico	6872 ± 1833.7	0.8 ± 0.01	1814 ± 425.7
opico	6714 ± 2590.8	0.8 ± 0.001	1384 ± 249.8
nano1	2167 ± 2065.8	3.0 ± 0.012	30627 ± 28456.1
nano2	274 ± 206.6	7.2 ± 0.017	51138 ± 52154.8
nano3	0.3 ± 1	14.6 ± 0.155	5.7 ± 1988.1

assessing the relationships among all predictor and response variables in a single analysis. Fitted site scores from the PCA were used to create a correlation triplot, thus the angles in the triplot between response and explanatory variables, and between the both the response and explanatory variables themselves, reflect their correlations. Permutation tests with 1000 iterations were conducted to assess the statistical significance of the RDA triplots. All statistical procedures were conducted using R statistical software version 3.5.1.

3. Results

3.1. FCM statistics and relationship to extracted Chl a

Phytoplankton cell counts (all samples pooled) measured by flow cytometry indicated average picophytoplankton (0.8 ± 0.01 μm) and NANO1 (3.0 ± 0.12 μm) abundance in the range of 10^3 cells mL^{-1}, average NANO2 (7.2 ± 0.17 μm) abundance was 10^2 mL^{-1}, and average NANO3 (14.6 ± 0.16 μm) was 10^1 mL^{-1} (Table 1). Heterotrophic bacteria (HBACT) averaged 0.5 ± 0.001 μm cell diameter and were abundant at 10^5 cells mL^{-1} (Table 1). Although picophytoplankton were numerically dominant, the NANO 2 size class of phytoplankton dominated the biovolume (ESV mL^{-1}) because of the elevated biovolume of each cell (e.g. larger cell diameter). On average, the biovolume (ESV mL^{-1}) of heterotrophic bacteria was greater than that of the picophytoplankton and of the same order of magnitude as that of the nanophytoplankton (Table 1).

Surface phytoplankton biovolume (ESV, μm^3 mL, determined by flow cytometry) was related to surface phytoplankton Chl *a* biomass (mg m^{-3}) in a 2nd order polynomial regression (log Chl *a* = −0.1661logESV + 0.1157logESV2 – 2.8716, r2 = 0.93, p < 0.001) (station averages). For pooled Kiholo and Kaloko data, the surface phytoplankton Chl *a*: biovolume ratio averaged 2.7 ± 1.94 μg Chl *a* mm^3, within the range reported by other studies (Felip and Catlan, 2000). We recognize that flow cytometry only measures a subset (pico- and nano-) phytoplankton and that not all sites samples were low Chl *a* areas dominated by these forms, (e.g. Kaloko fishpond (Fig. 1)).

3.2. Physical/chemical conditions at each site

Descriptive statistics generated for stations farthest from the main SGD source (e.g. 'offshore') indicated little difference in surface or bottom water parameters between sites (Table 2) whereas difference in fishponds and nearshore water were more pronounced. The salinity of Kiholo fishpond (6.3 ± 4.05) was lower than Kaloko fishpond (20.9 ± 3.15). Kiholo fishpond had elevated levels of NO_3 and PO_4 compared to Kaloko fishpond (Fig. 3 inset values). Outside the fishponds, the surface salinity gradient at Kiholo bay was detectable to at least 1.5 km from the main SGD source (Fig. 1). The initial 350 m of this gradient inside the lagoon through which groundwater flowed from the head (Fig. 1 (Sta 22)) to the inner bay area. Concentrations of NO_3, PO_4 and Si were negatively correlated with salinity at Kiholo, while ammonium was positively correlated with salinity (Fig. 3A–D). At Kaloko, similar patterns were observed outside the fishpond but were less pronounced, with reduced surface salinity detected adjacent to the fishpond wall, reflecting a source of groundwater at the opening in the wall (*makaha*) at the south end (Fig. 1, Sta 33), and just past the south end of the wall (Fig. 1, sta. 31). Nitrate and Si were negatively correlated with salinity at Kaloko.

3.3. Relationship between water quality and phytoplankton for combined dataset

For Kiholo, the permutation test of the RDA (R^2 = 21.8%) results indicated the relationships among the physical water quality parameters and the cell count response variables were statistically significant (F = 1.90, p < 0.05). RDA results indicated Nano1 was positively related to NH_4 and salinity, Nano2 was positively related to NO_3, Si, and PO_4. For Kaloko the permutation test of the RDA (R^2 = 83.7%%) results indicate the relationships among the psychical water quality parameters and the cell count response variables are statistically significant (F = 35.98, p < 0.01). RDA results indicate counts of Nano1 are positively related to chlorophyll *a* and negatively related to salinity. Nano2 is positively related to NH_4 and Pico exhibits a strong negative relationship to NO_3.

Overall from the RDA, including fishponds and the costal ocean combined, a negative relationship between salinity and inorganic nutrients was more strongly expressed at Kiholo. Both sites showed negative relationships between phytoplankton cell counts and salinity but at Kiholo it was larger cells (Nano2) showing this trend compared to smaller cells (Nano1) at Kaloko.

3.4. Comparisons of phytoplankton and heterotrophic bacteria in fishponds vs. ocean

Phytoplankton Chl *a* biomass (μg L^{-1}), biovolume (ESV mL^{-1}) and average cell size was significantly higher (p < 0.001) in the fishponds compared to the ocean at Kiholo and Kaloko sites (Fig. 5), but heterotrophic bacteria abundance differed between pond and ocean only at Kaloko (Fig. 5). Geometric mean (± se) phytoplankton abundance was 14.9 ± 1.59 μg Chl *a* L^{-1} at Kaloko fishpond (*n* = 16) and 2.2 ± 0.29 μg Chl *a* L^{-1} at Kiholo fishpond (*n* = 15).

Flow cytometric cell counts for each size class (Fig. 6) showed differences between ponds and ocean at each site, as well as in comparisons of like habitats between sites. Outside the fishponds at Kiholo (Fig. 6A) and Kaloko (Fig. 6B), the numerical abundance phytoplankton was dependent on category size class with similar slopes and intercepts, whereas only Kaloko fishpond (Fig. 6B) showed a dependence of phytoplankton numerical abundance on category size class but with a higher intercept than was seen outside the fishponds. The difference in the relative numerical abundance of picophytoplankton between Kiholo and Kaloko fishponds appears to drive the differences in regressions between these sites.

3.5. Phytoplankton and heterotrophic bacteria vs. salinity outside the fishponds

General additive models (GAMs) showed higher levels of phytoplankton and heterotrophic bacteria biomass parameters at Kiholo at brackish to high salinity (> 20), and lower values as salinity dropped below ~20 (Fig. 7A,B,D). This pattern was not evident in GAMs at Kaloko, perhaps due to the lower range of salinities present at this site (Fig. 7E and F,H). Rather, over the short range of salinities found in surface waters outside the fishpond at Kaloko, all parameters tended to increase at lower salinities (~24–30). Average phytoplankton cell size tended show higher values in brackish water at both sites (Fig. 7C,G). Flow cytometric cell counts of different phytoplankton size classes vs. salinity showed different relationships among size classes and sites

Table 2
Offshore conditions summarized as mean ± se at Kiholo and Kaloko. Surface and deep values are shown separately with sample size,n. salinity (ppt); NO_3, PO_4, NH_4 and Si (μmol L^{-1}); Chl *a*, mg m^{-3}; ESV (μm^3 mL^{-1} (phytoplankton)); AvgESD, (μm); Hbact (cells mL^{-1}); HESV,(μm^3 mL^{-1} (hetertrophic bacteria)).

	Surface > 1500 m		Surface ≥500 m		Deep ≥1500 m		Deep ≥500 m	
Parameter	n	Kiholo	n	Kaloko	n	Kiholo	n	Kaloko
Salinity	26	34.3 ± 0.10	19	34.4 ± 0.06	9	34.8 ± 0.06	9	34.8 ± 0.05
NO_3	27	1.5 ± 0.47	15	0.6 ± 0.23	11	0.7 ± 0.11	7	0.3 ± 0.09
PO_4	27	0.1 ± 0.02	15	0.0 ± 0.00	11	0.0 ± 0.01	7	0.0 ± 0.02
Si	27	6.6 ± 5.43	15	3.3 ± 2.02	11	0.4 ± 0.07	7	0.1 ± 0.10
NH_4	27	3.5 ± 0.44	15	0.0 ± 0.03	11	3.7 ± 1.04	7	0.1 ± 0.01
Chl *a*	17	0.13 ± 0.019	16	0.13 ± 0.030	10	0.09 ± 0.014	8	0.08 ± 0.019
Log ESV	27	4.8 ± 0.05	19	4.8 ± 0.05	10	4.7 ± 0.07	9	4.5 ± 0.10
AvgESD	27	1.4 ± 0.09	19	1.1 ± 0.05	11	1.3 ± 0.13	9	1.1 ± 0.08
Log HBACT	27	5.7 ± 0.03	19	5.8 ± 0.02	11	5.6 ± 0.10	9	5.7 ± 0.06
Log HESV	27	4.4 ± 0.02	19	4.5 ± 0.02	11	4.3 ± 0.08	9	4.4 ± 0.05

(Fig. 8). At Kiholo Bay, the picophytoplankton and nano1 size classes (Fig. 8A and B) class were positively correlated to salinity while the Nano2 (Fig. 8C) size class was not. At Kaloko, all size classes of phytoplankton were negatively correlated with salinity, albeit weakly.

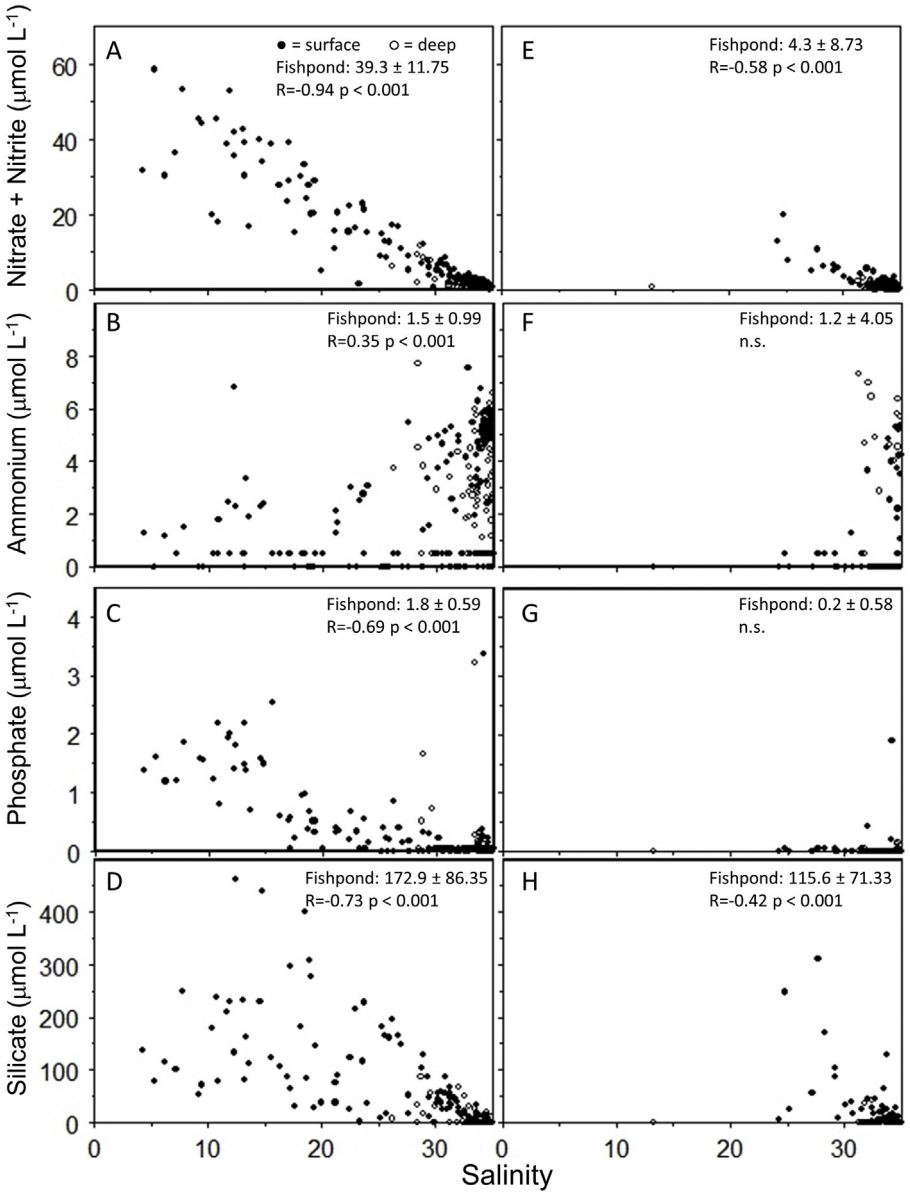

Fig. 3. Dissolved inorganic nutrient vs. salinity for surface (solid) and deep (open) samples. Average values for the same parameters within fishponds at each site are shown inset ± se. Correlation statistics for combined surface/deep ocean samples are shown below fishpond values. n.s = not significant.

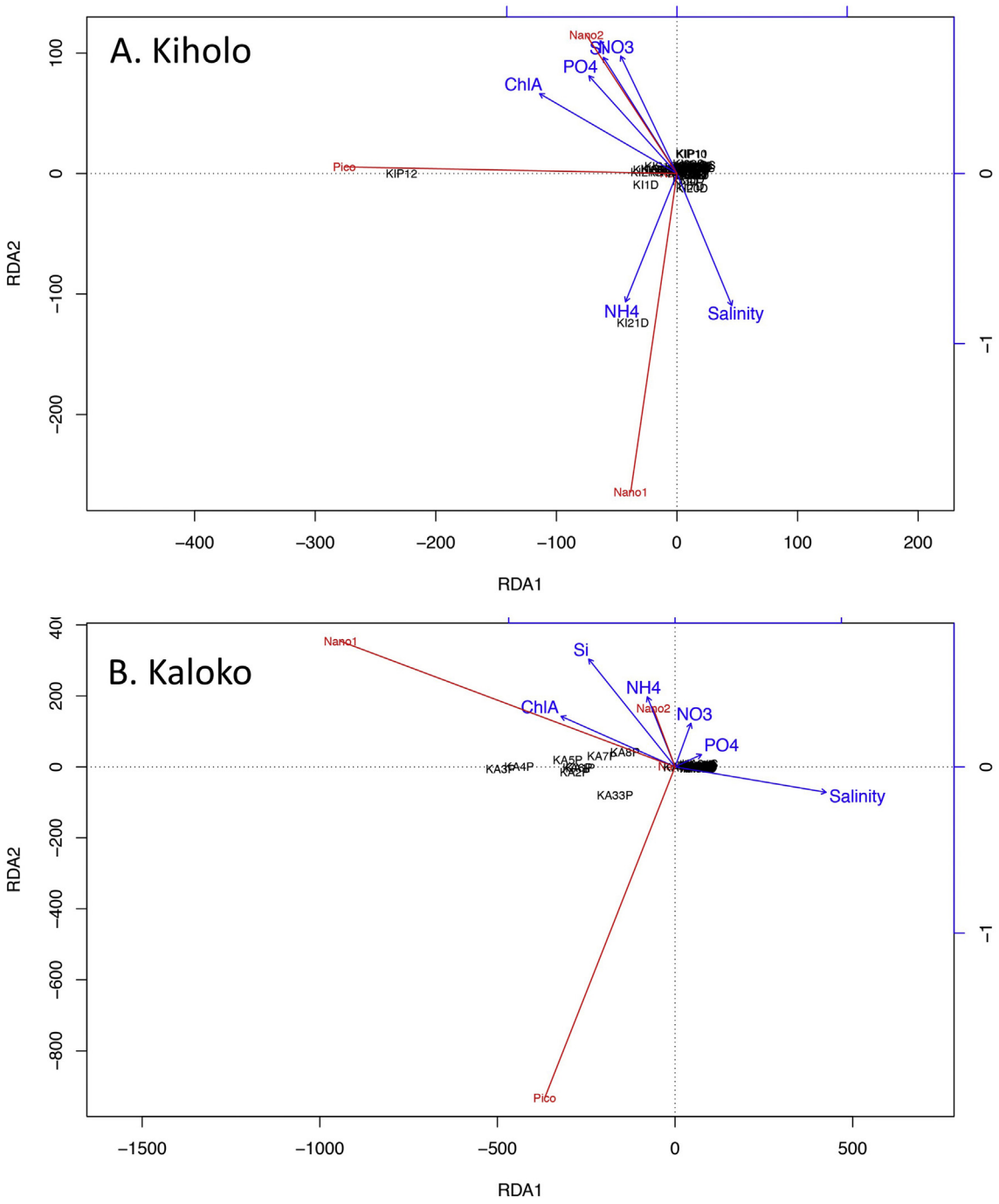

Fig. 4. Redundancy analyses of the total datasets (surface, deep, fishpond, ocean) for each location. Cell counts are shown in red, water quality variables are shown in blue.

3.6. Comparison of surface vs. deep water phytoplankton and heterotrophic bacteria

At Kiholo Bay, analyses of surface – deep differences in log ESV (phytoplankton biovolume) and AvgESD (average phytoplankton cell size) at stations having paired surface deep samples showed significantly elevated values in deep water at station 1, corresponding to the layer of Kiholo lagoon beneath the SGD pycnocline, and elevated values in surface water at several stations within the brackish portion of Kiholo bay (Sta. 5,6,8) (Fig. 9A). Average cell diameter was elevated in surface waters at station 5 and station 20 (Fig. 9B). Heterotrophic bacteria showed no difference between surface and bottom waters at any station at Kiholo (not shown).

At Kaloko, differences between surface and bottom waters were fewer. Only station 14 (~200 m from the wall opening, or *makaha*) showed significant differences in phytoplankton biovolume (Fig. 9C), and stations 14 and 16 showed significant differences in average cell size, both of which were elevated in surface waters (Fig. 9D).

4. Discussion

Nearshore phytoplankton communities are dynamically influenced by freshwater inputs from the land. Understanding the relationship between freshwater inputs and coastal phytoplankton dynamics is important to understanding changes in coastal marine ecosystems that might result from climate- or coastal development-driven changes in

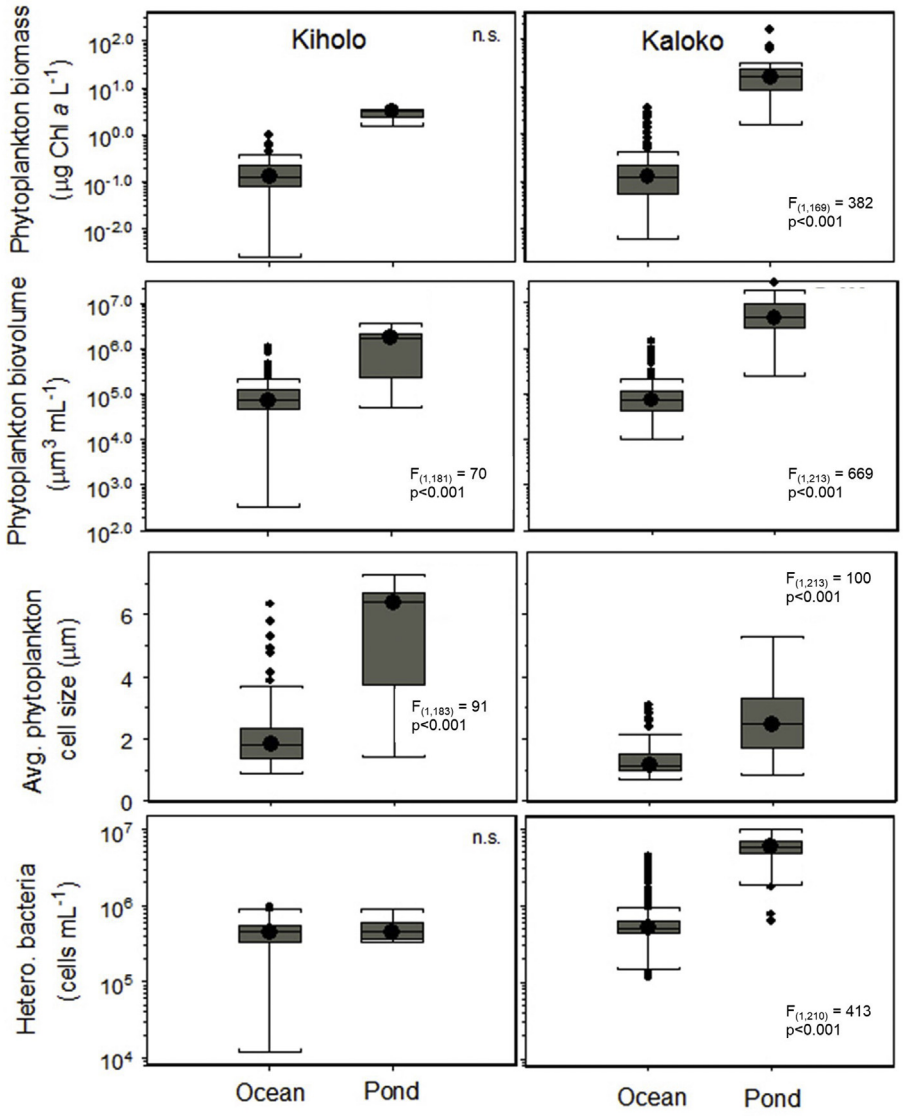

Fig. 5. Phytoplankton and heterotrophic bacteria comparisons between ocean and fishpond at (A–D) Kiholo and (E–H) Kaloko. The large circle in each box is the mean; the horizontal line in the box is the median. The top and bottom of the box is the 75th and 25th percentile, respectively. The top and bottom of the whisker caps represent the 95th and 5th percentiles, respectively. Small circles indicate data outside this range. Statistical results for pond – ocean comparisons are shown in the upper right of each graph.

freshwater inputs. This study showed the relationship between freshwater inputs, in the form of SGD, to the oligotrophic coastal ocean and phytoplankton and heterotrophic bacteria biomass and community composition. The main patterns we observed at the contrasting sites we studied can be summarized as (1) elevated phytoplankton biomass and larger average phytoplankton cell size (relative to the adjacent ocean) within groundwater-fed fishponds, (2) surface layer enhancement of phytoplankton biomass and average cell size in brackish water outside the fishponds, and (3) lower-layer enhancement of phytoplankton biomass beneath the strong SGD source in Kiholo lagoon.

4.1. Fishponds phytoplankton biomass

The sites we studied both were characterized by SGD inputs, negligible surface water inputs, and the presence of traditional Hawaiian fishponds that partially confined SGD to produce a zone of elevated productivity and brackish water adjacent to the coastal ocean. Thus, the influence of SGD on phytoplankton in the coastal ocean at these sites was modulated by the presence of fishponds. Kiholo and Kaloko fishponds had elevated phytoplankton abundance compared to the adjacent ocean, consistent with previous studies that have reported elevated phytoplankton Chl *a* biomass in Kaloko fishpond (Bienfang, 2007). No previous studies of Kiholo fishpond Chl *a* are available. Although a major fishpond existed historically at Kiholo, an 1859 lava flow filled most of it resulting in the present Kiholo Bay geomorphology including the lagoon (Young et al., 1977). The present day Kiholo fishponds are smaller, and our measurements show lower phytoplankton and heterotrophic bacteria biomass than Kaloko. Our and others' results support the conclusion that Kaloko fishpond is presently eutrophic: Kaloko fishpond Chl *a* was found to average 6 µg L^{-1} but ranged from < 1 to 48 µg L^{-1} over the annual cycle (Bienfang, 2007; Hoover and Gold, 2005), which is 1–2 orders of magnitude above the adjacent oligotrophic coastal ocean. Kaloko fishpond Chl *a* levels were similar to those observed in a known Hawaiian eutrophic environments, near the outfall site in Kaneohe Bay, O'ahu before sewage diversion (4.67 µg L^{-1}) (Smith et al., 1981). Kaloko fishpond heterotrophic bacterial abundance was approximately 10x higher than measurements reported for Station Aloha in the North Pacific Ocean (Landry and Kirchman, 2002) or offshore measurement made in the present study.

Kaloko fishpond, formed approximately 300 years ago by the

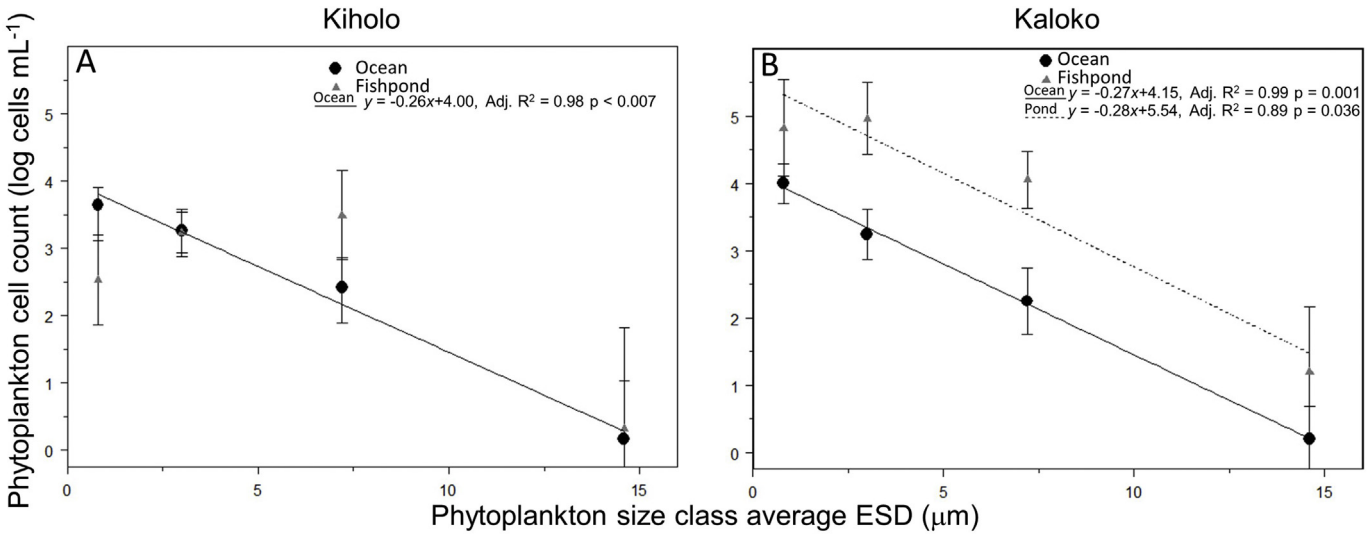

Fig. 6. Phytoplankton cell counts vs. size class average ESD for pond and ocean at (A) Kiholo and (B) Kaloko. The linear regression for Kiholo fishpond was not significant.

construction of a semi-permeable stone wall that captured coastal and submarine groundwater discharge within a natural embayment forming a brackish inner zone where fish could be raised for human consumption (Bond and Gmirkin, 2003), is an important cultural asset of Hawai'i Island and Hawaiian cultural history. It is unclear whether the current eutrophic status of the fishpond reflects historical conditions, but this is not likely the case. Long-time residents of the area say that Kaloko fishpond was clearer and cleaner 50–60 years ago, (R. Most, pers. comm.), and there is some evidence that N concentrations in SGD have increased in West Hawaii groundwater over the last 2-3 decades (Hoover and Gold, 2005; Parsons et al., 2008). *A Collection of Family Traditions Describing Customs, Practices and Beliefs of the Families and Lands of Kaloko and Honokohau, North Kona, Island of Hawaii* (Maly, 2006), provides an account of the pond water turning red approximately once a month, which prompted swimming bans and was attributed to the menstrual cycle of the *mo'o*, or guardian spirit of the pond (Maly, 2006). Whether or not these accounts reflect blooms of 'red tide' phytoplankton consistent with the pond's eutrophic status, or if other potential harmful phytoplankton and/or bacteria are present in this fishpond, are important areas for future research.

4.2. Phytoplankton and bacteria outside the fishponds

Offshore phytoplankton assemblages were dominated by picophytoplankton including *Synechococcus*, as observed in other studies of the region reviewed by Landry and Kirtchman (2002). Our offshore counts of *Synechococcus* ($6.7 \times 10^3 \pm 2.59 \times 10^3$ cells mL^{-1}) were slightly higher than offshore surface waters in the lee of O'ahu (2.0×10^3 cells mL^{-1} Brown et al., 2008), Station Aloha to the north of O'ahu (1.7×10^3 cells mL^{-1}), and the western equatorial Pacific (2.3×10^3 cells mL^{-1}) (Landry and Kirchman, 2002). Our *Synechococcus* counts were more similar to the HNLC equatorial Pacific (9.8×10^3 cells mL^{-1}) (Landry and Kirchman, 2002) and an oceanic station outside Kaneohe Bay, O'ahu (8×10^3 cells per mL, Cox et al., 2006). *Synechococcus* counts from Kaloko fishpond (1.1×10^5 cells per mL), on the other hand, were elevated in our study and similar to observations made in Kaneohe Bay ($\sim 3 \times 10^5$ cells mL^{-1}), despite total Chl *a* levels within Kaneohe Bay that were lower (0.6–1.4 μg L^{-1}, Cox et al., 2006) than in Kaloko fishpond. Variability of *Synechococcus* across this range of environments thus spanned 10^2 cells per mL (Kiholo fishpond) to 10^5 cells per mL (*i.e.* between Kaloko fishpond and Kaneohe Bay) despite significant differences in total Chl *a* biomass between these latter environments.

Our observations at Kiholo and Kaloko extend on others' observations of elevated Chl *a* phytoplankton biomass 'in-plume' vs. 'out-of-plume' at these sites (Johnson and Wiegner, 2014) by detailing the extent of elevated biomass and changes to the community composition at each site relative to the full salinity gradient. The pattern of phytoplankton biomass we observed at Kaloko likely reflects simple export of eutrophic fishpond water through the *makaha*. This conclusion is supported by the low salinity (Fig. 1) and nutrient levels (Fig. 3E–H) outside Kaloko fishpond. Expelled fishpond water is expected to have nutrients drawn down by the high phytoplankton biomass in the pond. Further, elevated heterotrophic bacteria (Fig. 7H) observed just outside the *makaha* reflect conditions seen inside the fishpond. An important area for future research and monitoring is understanding the effect of eutrophic Kaloko fishpond water export on the adjacent oligotrophic ocean and coral reef ecosystem, which is becoming an increasingly important issue where interest in pond aquaculture is growing (Herbeck and Unger, 2013).

Previous studies of the effects of SGD on phytoplankton emphasize changes to the community composition in addition to biomass (Alvarez-Gongora and Herrera-Silveira, 2006; Troccoli-Ghiaglia et al., 2010; Blanco et al., 2008), and our measurements of phytoplankton size structure suggest changes to community composition both inside and outside of the fishponds, as well as between sites (Figs. 4–8). At Kiholo, plots of NO_3 and PO_4 vs. salinity outside the fishponds suggest non-conservative mixing (Fig. 3A,C), as has previously been described by Johnson and Wiegner (2014), consistent with the idea that SGD nutrients support phytoplankton growth. General additive model results for Chl *a* and ESV support elevated phytoplankton biomass between apx. 20–25 salinity at Kiholo (Fig. 7A and B), and the more-pronounced increase in average cell size at this same salinity range (Fig. 7C) supports the conclusion of a change in phytoplankton community composition outside the fishponds at Kiholo. Our calculation of average cell size integrates the relative abundance of different size classes of phytoplankton, and since we observed a decline in picophytoplankton, but not the larger class of nanophytoplankton, in this salinity region (Fig. 8A–C), we conclude that the change in phytoplankton community composition here (Fig. 7C) was driven by the loss of picophytoplankton at lower salinities despite elevated nutrient levels. This agrees with results of Chamberlain et al. (2014) who showed that additions of groundwater to ocean water resulted in declines of Hawaii Island populations of planktonic cyanobacteria, and Lecher et al. (2015) who saw no significant effect of groundwater amendments on picophytoplankton in Monterey Bay. Garces et al. (2011) did see stimulation of

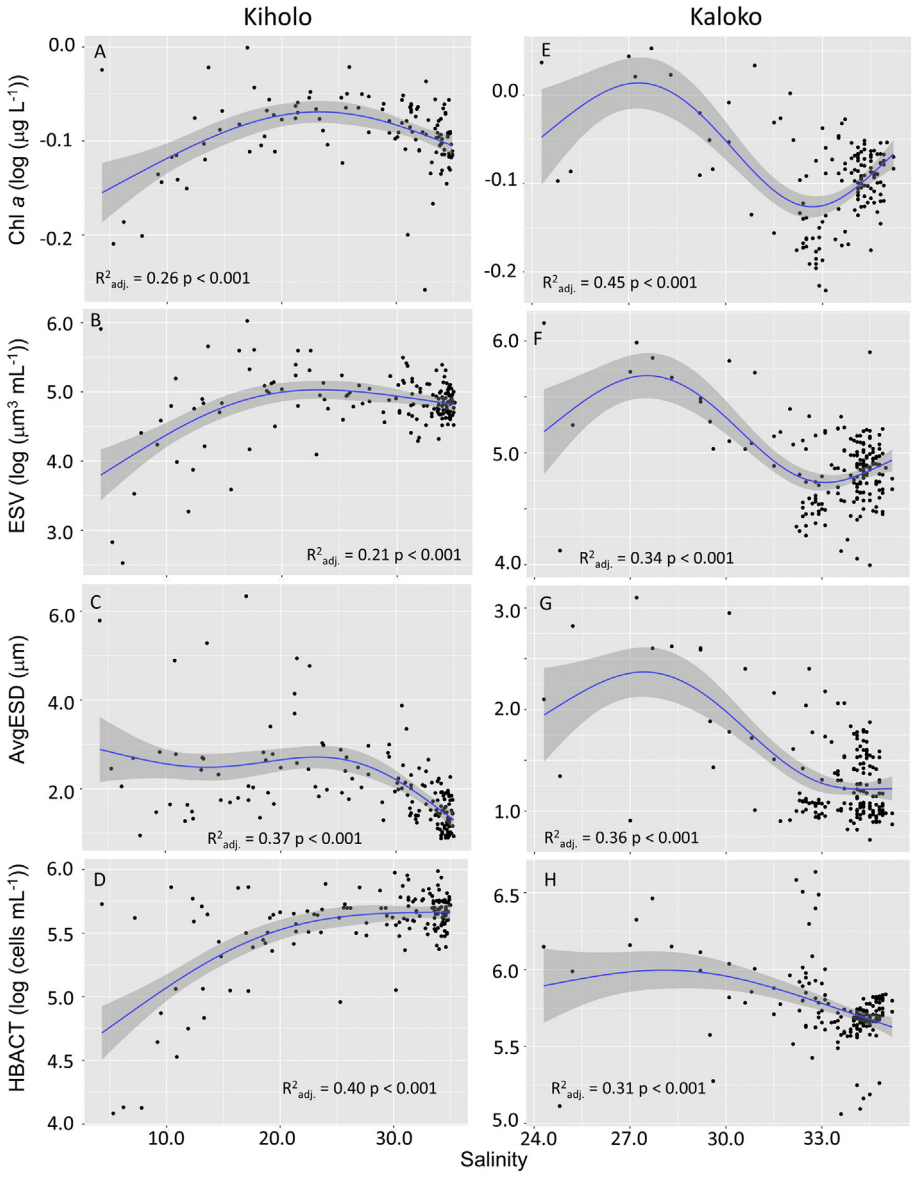

Fig. 7. Surface phytoplankton parameters (Chl *a*, FCM biovolume, and average community cell size) and heterotrophic bacteria cell counts vs. salinity for waters outside the fishponds at Kiholo and Kaloko.

Synechococcus in short-term experimental groundwater amendments in oligotrophic Mediterranean waters, but also a strong effect of nutrient enrichment on diatoms that were not typical members of the phytoplankton for the season in which their experiments were performed.

Ocean residence time in West Hawaii has been estimated at < 1.6 d based on isotope ratios studies (Knee et al., 2008), which is short enough to limit phytoplankton accumulations as phytoplankton growth rates are typically 1–2 divisions d^{-1}. Although residence time was not measured in this study, our observations at Kiholo Bay are consistent with observations of Waters et al. (2015) who reported higher Chl *a* associated with older waters (range 3–11 days) in the inner region of Kiholo Bay. Interestingly, heterotrophic bacterial biomass did not peak in this area of Kiholo Bay suggesting a differential effect of SGD on autotrophic biomass (Fig. 7D). The role that coastal ocean residence time plays in modulating the response of phytoplankton to SGD nutrients in coastal Hawaiian environments, or any coastal environment associated with ocean islands having low coastal residence times, remains a critical area for future research.

Hawaiian environments influenced by SGD often show salinity stratification (Johnson et al., 2008), and this is the case for these sites as well (Fig. 1), with Kiholo Bay in particular showing a strong halocline approximately 1 m below the surface. The subsurface accumulations of phytoplankton found beneath the strong SGD source in Kiholo lagoon are similar to observations made previously by Bienfang and Johnson (1980) in Kaloko-Honokohau Harbor. Such sites likely serve as important biological 'hot spots', as has been described for so-called plankton 'thin-layers' observed throughout the world's oceans (Durham and Stocker, 2012). Strong flushing at the head of Kiholo lagoon appeared to dilute surface phytoplankton and bacteria, similar to observations noted for the SGD source in Kaloko-Honokohau Harbor (Bienfang and Johnson, 1980). This suggests a hydrologic forcing of subsurface accumulations of phytoplankton in the lagoon and other areas where SGD sources are strong. Understanding the mechanisms underlying such bottom accumulations, and their role in local trophodynamics is an important area for future research. In the context of coastal management and monitoring, these sites suggest the importance of sampling sub-surface waters when monitoring for a biological response to nutrification and compliance with state water quality criteria in these SGD-influenced environments.

In general, we observed an association throughout our study of

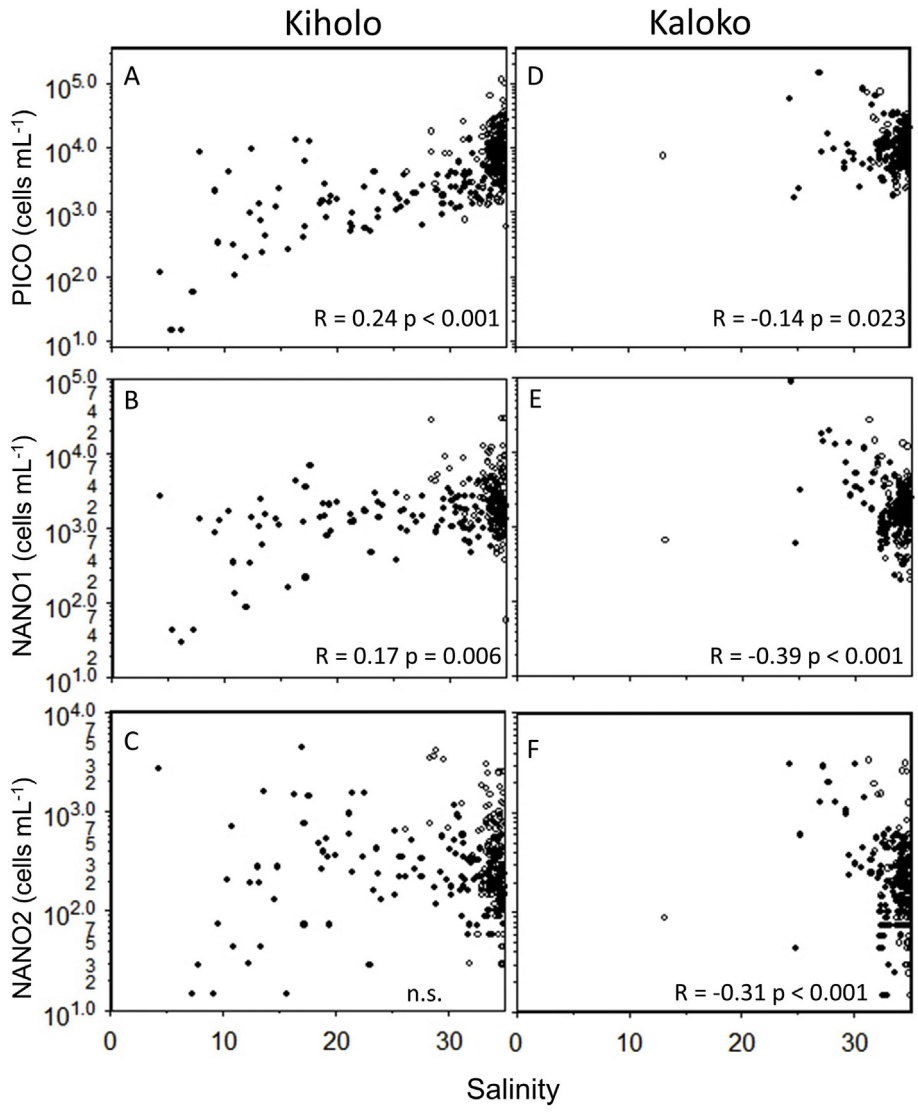

Fig. 8. Flow cytometric cell counts of different size classes of phytoplankton vs. salinity at Kiholo and Kaloko. Closed symbols are surface samples, open symbols are deep water samples. Pearson R and p-values are shown on each plot (surface and deep combined).

larger average phytoplankton cell size accompanying elevated phytoplankton biomass, including both fishponds (Fig. 5), the surface Kiholo Bay brackish region (Fig. 7), and the lower layer of the Kiholo lagoon (Fig. 9). This association was also present in our RDA of the combined (pond and ocean) dataset that showed relationships between Chl *a* and specific phytoplankton size classes (Fig. 4). This was consistent with the expected phytoplankton biomass – community size structure relationships (Chisholm, 1992; Thingstad, 1997; Irwin et al., 2006), wherein higher phytoplankton biomass results from larger cells (nanophytoplankton) growing 'over' a steady background of picophytoplankton. Similar shifts in biomass and composition have been observed in cyclonic eddies that bring nutrients to the oligotrophic surface ocean in the lee of Hawaii Island (Brown et al., 2008). Ecologically, this shift in the size classes of phytoplankton associated with increased biomass at SGD sites suggests changes in the trophic structure of the food web (Thingstad, 1997), and strongly points to the need for further studies of the effects of SGD on microzooplankton and their role in the fate of primary production at SGD sites.

Phytoplankton are important contributors to primary production in the coastal ocean around Hawaii Island (Wabnitz et al., 2010) and other tropical island/atoll ecosystems where natural and/or anthropogenic forces modulating freshwater inputs can enhance phytoplankton biomass (Gove et al., 2016). Traditional Hawaiian fishponds represent an important aspect of Hawaiian cultural history and continue to provide valuable cultural and food resource to communities that undertake restoration of these often-degraded systems. Although coral reef communities depend upon phytoplankton production they can also be threatened by over-abundance of phytoplankton (Smith et al., 1981; Bell et al., 2014). It is important that we better understand the linkages between freshwater inputs, nutrients, phytoplankton, traditional fishponds and coastal communities in the context of plans to conserve these culturally and ecologically important environments in the face of anthropogenic development and climate change that represent major threats to their functioning and existence (Knowlton and Jackson, 2008).

Acknowledgements

This material is based upon work supported by the National Science Foundation under award #0833211, the CREST-PRF Award #1720706, and EPSCoR Program Award OIA #1557349. Any opinions, findings, and conclusions or recommendations expressed in this material are those of the authors and do not necessarily reflect the views of the National Science Foundation. The authors thank Drs. Tracy Wiegner,

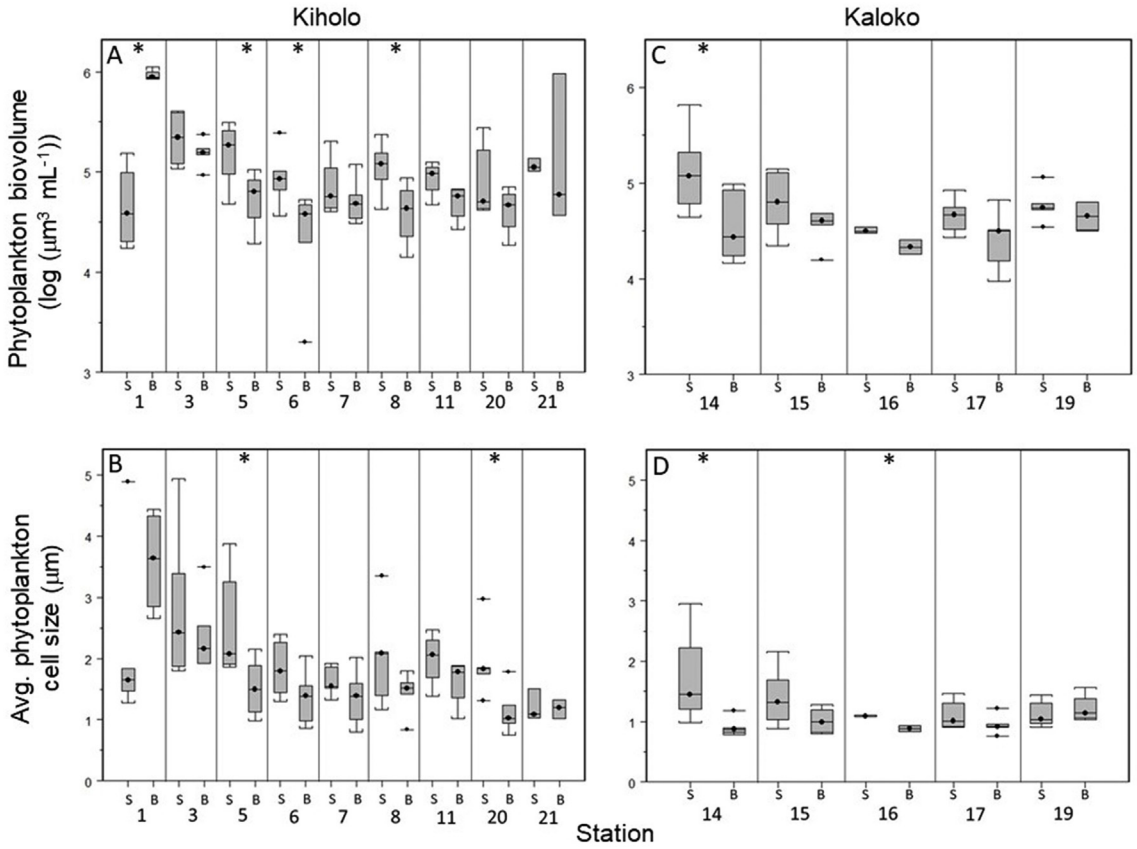

Fig. 9. Comparison of surface (S) and bottom (B) samples at station where paired S/B samples were taken. (*) indicates significant difference ($p < 0.05$) between pooled surface/bottom samples for a given station.

Jim Beets, and Steven Colbert as well as associated undergraduate and graduate students for their assistance.

Appendix A. Supplementary data

Supplementary data to this article can be found online at https://doi.org/10.1016/j.ecss.2019.01.021.

References

Alvarez-Gongora, C., Herrera-Silvera, J.A., 2006. Variations of phytoplankton community structure related to water quality trends in a tropical karstic coastal zone. Mar. Pollut. Bull. 52, 48–60.

Bell, P.R.F., Ehmetri, I., Lapointe, B.F., 2014. Evidence of large scale chronic eutrophication in the Great Barrier Reef: quantification of Chlorophyll *a* thresholds for sustaining coral reef communities. Ambio. https://doi.org/10.1007/s13280-013-0443-1.

Bienfang, P., 1980. Water quality characteristics of Honokohau Harbor, a subtropical embayment affected by groundwater intrusion. Pac. Sci. 34 (3), 279–281.

Bienfang, P., 2007. Assess Nutrient Sources, Fluxes, and Water Quality of Ponds within the Kaloko-Honokohau National Historical Park, Final Report. 2007. Unpublished Report-2186087. Hawai'i-Pacific Islands Cooperative Ecosystem Studies Unit. University of Hawai'i at Manoa, Honolulu, Hawai'i.

Bienfang, P., Johnson, W., 1980. Planktonic properties of Honokohau Harbor: a nutrient-enriched subtropical embayment. Pac. Sci. 34 (3), 293–300.

Blanco, A.C., Nadaoka, K., Yamamoto, T., 2008. Planktonic and benthic microalgal community composition as indicators of terrestrial influence on a fringing reef in Ishigaki Island, Southwest Japan. Mar. Environ. Res. 66, 520–535.

Bond Jr., S., Gmirkin, R., 2003. Restoring part of Hawaii's past: Kaloko fishpond restoration. Ecol. Restor. 21 (4), 284–289.

Borcard, D., Gillet, F., Legendre, P., 2011. Numerical Ecology with R. Springer, New York.

Brown, S.L., Landry, M.R., Selph, K.E., Yang, E.J., Rii, Y., Bidigare, R.R., 2008. Diatoms in the desert: plankton community response to a mesoscale eddy in the subtropical North Pacific. Deep-Sea Research II 55, 1321–1333.

Burnett, W., Bokuniewicz, H., Huettel, M., Moore, W., Taniguchi, M., 2003. Groundwater and pore water inputs to the coastal zone. Biogeochemistry 66, 3–33.

Burnett, W.C., Aggarwal, P.K., Aureli, A., Bokuniewicz Cable, J.E., Charette, M.A., Kontar, E., Krupa, S., Kulkarni, K.M., Loveless, A., Moore, W.S., Oberdorfer, J.A., Oliveira, J., Ozyurt, N., Povinec, P., Privitera, A.M.G., Rajor, R., Ramessur, R.T., Scholten, J., Stieglitz, T., Taniguchi, M., Turner, J.V., 2006. Quantifying submarine groundwater discharge in the coastal zone via multiple methods. Sci. Total Environ. 367, 498–543.

Calbet, A., Landry, M.R., 2004. Phytoplankton growth, microzooplankton grazing, and carbon cycling in marine systems. Limnol. Oceanogr. 49, 51–57.

Calbet, A., Saiz, E., 2005. The ciliate-copepod link in marine ecosystems. Aqatic Microbial Ecology 38, 157–167.

Chamberlain, S.D., Kaplan, K.A., Modanu, M., Sirianni, K.M., Annandale, S., Hewson, I., 2014. Biogeography of planktonic and benthic cyanobacteria in coastal waters of the Big Island, Hawaii. FEMS Microbiol. Ecol. 89, 80–88.

Chisholm, S.W., 1992. Phytoplankton size. In: Falkowski, P.G., Woodhead, A.D. (Eds.), Primary Productivity and Biogeochemical Cycles in the Sea.

Cox, E.F., Ribes, M., Kinzie III., R.A., 2006. Temporal and spatial scaling of planktonic responses to nutrient inputs into a subtropical embayment. Mar. Ecol. Prog. Ser. 324, 19–35.

DeVerse, K., 2006. Appendix A: kaloko-honokohau national historical park resource overview. In: HaySmith, L., Klasner, F.L., Stephens, S.H., Dicus, G.H. (Eds.), Pacific Island Network Vital Signs Monitoring Plan. Natural Resource Report NPS/PACN/NRR—2006/003. National Park Service, Fort Collins, Colorado.

Dimova, N., Swarzenski, P., Dulaiova, H., Glenn, C., 2012. Utilizing multichannel electrical resistivity methods to examine the dynamics of the fresh water–seawater interface in two Hawaiian groundwater systems. J. Geophys. Res. 117. https://doi.org/10.1029/2011JC007509.

Dollar, S.J., Atkinson, M.J., 1992. Effects of nutrient subsidies from groundwater to nearshore marine ecosystems off the island of Hawaii. Estuar. Coast Shelf Sci. 35, 409–424.

Durham, W.M., Stocker, R., 2012. Thin phytoplankton layers: characteristics, mechanisms, and consequences. Ann. Rev. Mar. Sci. 4, 177–207.

Fabricus, K.E., 2005. Effects of terrestrial runoff on the ecology of corals and coral reefs: review and sysnthesis. Mar. Pollut. Bull. 50, 125–146.

Felip, M., Catalan, J., 2000. The relationship between phytoplankton biovolume and chlorophyll in a deep oligotrophic lake: decoupling in their spatial and temporal maxima. J. Plankton Res. 22 (1), 91–105.

Garces, E., Basterretxea, G., Tovar-Sanchez, A., 2011. Changes in microbial communities in response to submarine groundwater input. Mar. Ecol. Prog. Ser. 438, 47–58.

Garrison, G.H., Glenn, C.R., Mcmurty, G.M., 2003. Measurement of submarine groundwater discharge in kahana bay, oahu, Hawaii. Limnol. Oceanogr. 48, 920–928.

Giambelluca, T.W., Chen, Q., Frazier, A.G., Price, J.P., Chen, Y.-L., Chu, P.-S., Eischeid, J.K., Delparte, D.M., 2013. Online rainfall atlas of Hawai'i. Bull. Am. Meteorol. Soc. 94, 313–316. https://doi.org/10.1175/BAMS-D-11-00228.1.

Gobler, C.J., Sanudo-Wilhelmy, S.A., 2001. Temporal variability of groundwater seepage

and brown tide blooms in a Long Island embayment. Mare. Ecol. Progr. Ser. 217, 299–309.
Goericke, R., 2011. The size structure of phytoplankton – what are the rules? CALCOFI (Calif. Coop. Ocean. Fish. Investig.) Rep. 52, 198–204.
Gove, J.M., McMannus, M.A., Neuheimer, A.B., Polovina, J.J., Drazen, J.C., Smith, C.R., Merrifield, M.A., Friedlander, A.M., Ehses, J.S., Young, C.W., Dillon, A.K., Williams, G.J., 2016. Near-island biological hotspots in barren ocean basins. Nat. Commun. 7, 10581. https://doi.org/10.1038/ncomms10581.
Herbeck, L.S., Ungerer, D., 2013. Pond aquaculture effluents traced along back-reef waters by standard water quality parameters, d15N in suspended matter and phytoplankton bioassays. Mar. Ecol. Prog. Ser. 478, 71–86.
Herrera-Silveira, J.A., 1998. Nutrient-phytoplankton production relationships in a groundwater-influenced lagoon. Aquat. Ecosys. Health Manag. 1, 373–385.
Hoover, D., Gold, C., 2005. Assessment of Coastal Water Resources and Watershed Conditions in Kaloko-Honokohau National Historic Park. National Park Service, U.S. Dept. of Interior, Hawaii Technical Report NPSNRWRD/NRTR-2005/344.
Irwin, A.J., Finkel, Z.V., Schofield, O.M.E., Falkowski, P.G., 2006. Scaling up from nutrient physiology to the size structure of phytoplankton communities. J. Plankton Res. 28 (5) 459-371.
Johannes, R.E., 1980. The ecological significance of the submarine discharge of groundwater. Mar. Ecol. 3, 365–373.
Johnson, E.E., Wiegner, T.N.W., 2014. Surface water metabolism potential in groundwater-fed coastal waters of Hawaii Island, USA. Estauries and Coasts 37, 712–723.
Johnson, A.G., Glenn, C.R., Burnett, W.C., Peterson, R.N., Lucey, P.G., 2008. Aerial infrared imaging reveals large nutrient-rich groundwater inputs to the ocean. Geophys. Res. Lett. 35, L15606.
Karl, D.M., Bidigare, R.R., Leitler, R.M., 2002. Sustained and aperiodic variability in organic matter production and phototrophic microbial community structure in the North Pacific Subtropical Gyre. In: Williams, P.J. le B., Thomas, D.N., Reynold, C.S. (Eds.), Phytoplankton Productivity – Carbon Assimilation in Marine and Freshwater Ecosystems. Blackwell Science.
Kikuchi, W.K., 1976. Prehistoric Hawaiian fishponds. Science 193, 295–299.
Kim, G., Lee, K.-K., Park, K.-S., Hwang, D.-W., Yang, H.-S., 2003. Large submarine groundwater discharge (SGD) from a volcanic island. Geophys. Res. Lett. 30.
Kim, G., Ryu, J.-W., Yang, H.-S., Yun, S.-T., 2005. Submarine groundwater discharge (SGD) into the Yellow Sea revealed by 228Ra and 226Ra isotopes: implications for global silica fluxes. Earth Planet. Sci. Lett. 237, 156–166.
Kim, G., Ryu, J.-W., Hwang, D.-W., 2008. Radium tracing of submarine groundwater discharge (SGD) and associated nutrient fluxes in a highly-permeable bed coastal zone, Korea. Mar. Chem. 109, 307–317.
Kim, G., Kim, J.-S., Hwang, D.-W., 2011. Submarine groundwater discharge from oceanic islands standing in oligotrophic oceans: implications for global production and organic carbon fluxes. Limnol. Oceanogr. 56 (2), 673–682.
Knee, K.L., Street, J.H., Grossman, E.E., Paytan, A., 2008. Submarine ground-water discharge and fate along the coast of kaloko-honokōhau national historical park, island of Hawai'i – Part 2, spatial and temporal variations in salinity, radium-isotope activity, and nutrient concentrations in coastal waters, December 2003-April 2006. U.S. Geological Survey Scientific Investigations, pp. 31p Report 2008-5128.
Knee, K.L., Street, J.H., Grossman, E.E., Boehm, A.B., Paytan, A., 2010. Nutrient inputs to the coastal ocean from submarine groundwater in a groundwater-dominated system: relation to land-use (Kona Coast, Hawaii, USA). Limnol. Oceanogr. 55, 1105–1122.
Knowlton, N., Jackson, J.B.C., 2008. Shifting baselines, local impacts, and global change on coral reefs. PLoS Biol. 6 (2), e54. https://doi.org/10.1371/journal.pbio.0060054.
Landry, M.R., Kirchman, D.L., 2002. Microbial community structure and variability in the tropical pacific. Deep-sea Research II 49, 2669–2693.
Landry, M.R., Haas, L.W., Fagerness, V.L., 1984. Dynamics of microbial plankton communities: experiments in Kaneohe Bay, Hawaii. Mar. Ecol. Prog. Ser. 16, 127–133.
Lapointe, B.E., O'connell, J.D.O., Garrett, G.S., 1990. Nutrient couplings between on-site sewage disposal systems, groundwaters, and nearshore surface waters of the Florida Keys. Biogeochemistry 10, 289–307.
Laws, E.A., Brown, D., Peace, C., 2004. Coastal water quality in the Kihei and Lahaina districts of the Island of Maui, Hawaiian Islands. Impacts from physical habitat and groundwater seepage: implications for water quality standards. Int. J. Environ. Pollut. 22, 531–546.
Lecher, A.L., Mackey, K., Kudela, R., Ryan, J., Fisher, A., Murray, J., Paytan, A., 2015. Nutrient loading through submarine groundwater discharge and phytoplankton growth in Monterey Bay, CA. Environ. Sci. Technol. 49, 6665–6673. https://doi.org/10.1021/acs.est.5b00909.
Lee, Y.-W., Kim, G., 2007. Linking groundwater-borne nutrients and dinoflagellate red-tide outbreaks in the southern sea of Korea using a Ra tracer. Estuar. Coast Shelf Sci. 71, 309–317.
Lee, Y.-W., Kim, G., Lim, W.-A., Hwang, D.-W., 2010. A relationship between groundwater-born nutrients traced by Ra isotopes and the intensity of dinoflagellate red-tides occurring in the southern sea of Korea. Limnol. Oceanogr. 55 (1), 1–10.
Li, W.K.W., Zohary, T., Yacobi, Y.Z., Wood, A.M., 1993. Ultraphytoplankton in the eastern Mediterranean Sea: towards deriving phytoplankton biomass from flow cytometric measurements of abundance, fluorescence, and light scatter. Mar. Ecol. Prog. Ser. 102, 79–87.
Maly, K., Maly, O., 2006. He Wahi Moʻolelo No Puʻuwaʻawaʻa a Me Nāpuʻu O Nā Kona: A Collection of Cultural and Historical Accounts of Puʻu Waʻawaʻa and the Nāpuʻu Region – District of Kona, on the Island of Hawai'i. Kumu Pono Associates LLC, HiHTEF116-Puʻu Waʻawaʻa (123006a).
Marsh, J.A., 1977. Terrestrial Inputs of Nitrogen and Phosphorus on Fringing Reefs of Guam. pp. 331–336 Proceedings, Third International Coral Reef Symposium.
Medina-Gomez, I., Herrera-Silveira, J.A., 2006. Primary production dynamics in a pristine groundwater influenced coastal lagoon of the Yucatan Peninsula. Cont. Shelf. Res. 26, 971–986.
Moore, W.S., 1999. The subterranean estuary: a reaction zone of ground water and sea water. Mar. Chem. 65, 111–125.
Moosdorf, N., Stieglitz, T., Waska, H., Dürr, H., Hartmann, J., 2014. Submarine groundwater discharge from tropical islands: a review. Grundwasser 20, 5367.
Morales-Ojeda, S.M., Herrera-Silveira, J.A., Montero, J., 2010. Terrestrial and oceanic influence on spatial hydrochemistry and trophic status in subtropical marine nearshore waters. Water Res. 44, 5949–5964.
Nixon, S.W., et al., 2007. Anthropogenic enrichment and nutrients in some tropical lagoons of Ghana, West Africa. Ecol. Appl. 17, 144–164.
Odebrecht, C., Du Preez, D.R., Abreu, P.C., Campbell, E.E., 2014. Surf zone diatoms: a review of the drivers, patterns, and role in sandy beaches food chains. Estuar. Coast Shelf Sci. 150, 24–35.
Oki, D.S., Tribble, G.W., Souza, W.R., Bolke, E.L., 1999. Ground water resources in kaloko-honokohau national historical park, island of Hawaii, and numerical simulations of ground-water withdrawls. Report No. USGS Water-Resurces Investigations Report, pp. 99–4070.
Paerl, H.W., 1997. Coastal eutrophication and harmful algal blooms: importance of atmospheric deposition and groundwater as 'new' nitrogen and other nutrient sources. Limnol. Oceanogr. 42, 1145–1165.
Parsons, M.L., Walsh, W.J., Settlemier, C.J., White, D.J., Ballauer, J.M., Ayotte, P.M., Osada, K.M., Carman, B., 2008. A multivariate assessment of the coral ecosystem health of two embayments on the lee of the island of Hawai 'i. Mar. Pollut. Bull. 56, 1138–1149.
Paytan, A., Shelenbarger, G.G., Street, J.H., Gonneea, M.E., Davis, K., Young, M.B., Moore, W.S., 2006. Submarine groundwater discharge: an important source of new inorganic nitrogen to coral reef ecosystems. Limnol. Oceanogr. 51, 343–348.
Peterson, R., Burnett, W., Glenn, C., Johnson, A., 2009. Quantification of point-source groundwater discharges to the ocean from the shoreline of the Big Island. Hawaii. Limnol. Oceanogr. 54, 890–904.
Rodellas, V., Garcia-Orellana, Tovar-Sánchez, A., Basterretxea, G., López-Garcia, J.M., Sánchez-Quiles, D., Garcia-Solsona, E., Masqué, P., 2014. Submarine groundwater discharge as a source of nutrients and trace metals in a Mediterranean bay (Palma Beach, Balearic Islands). Mar. Chem. 160, 56–66.
Shellenbarger, G.G., Monismith, S.G., Genin, A., Paytan, A., 2006. The importance of submarine groundwater discharge to the nearshore nutrient supply in the Gulf of Aqaba (Israel). Limnol. Oceanogr. 51, 1876–1886.
Slomp, C., Van Cappellen, P., 2004. Nutrient inputs to the coastal ocean through submarine groundwater discharge: controls and potential impact. J. Hydrol. 295, 64–86.
Smith, S.V., Kimmerer, W.J., Laws, E.A., Brock, R.E., Walsh, T.W., 1981. Kaneohe Bay sewage diversion experiment: perspectives on ecosystem responses to nutritional perturbation. Pac. Sci. 35, 279–395.
Street, J.H., Knee, K.L., Grossman, E.E., Paytan, A., 2008. Submarine groundwater discharge and nutrient additions to the coastal zone and coral reefs of leeward Hawai'i. Mar. Chem. 109, 355–376.
Thingstad, T.F., 1997. A theoretical approach to structuring mechanisms in the pelagic food web. Hydrobiologia 363, 59–72.
Tribble, G., 2008. Groundwater on tropical pacific islands - understanding a vital resource. USGS Circular 1312, 35.
Troccoli-Ghinaglia, L., Herrera-Silveira, J.A., Comin, F.A., Diaz-Ramos, J.F., 2010. Phytoplankton community variation in tropical coastal area affected where submarine groundwater occurs. Cont. Shelf Res. 30, 2082–2091.
Valiela, I., Costa, J., Foreman, K., Teal, J.M., Howes, B., Aubrey, D., 1990. Transport of groundwater-borne nutrients from watersheds and their effects on coastal waters. Biogeochemistry 10, 177–197.
Wabnitz, C.C.C., Balaaz, G., Beavers, S., Bjorndal, K.A., Bolten, A.B., Christensen, V., Hargrove, S., amd Pauly, D., 2010. Ecosystem structure and processes at Kaloko, focusing on the role of herbivoes, including the green sea turtle *Chlelonia mydas*, in reef resilience. Mar. Ecol. Prog. Ser. 420, 27–44.
Waters, C., 2015. Variability in Submarine Groundwater Discharge Composition and the Fate of Groundwater Delivered Nutrients at Kīholo Bay and Honokōhau Habor, North Kona District, Hawai'i (Master's Thesis). University of Hawai'i at Mānoa, Honolulu, Hawai'i.
Young, R.H.F., Kay, A.E., Lau, S.L., Stroup, E.D., Dollar, S.J., Fellows, D.P., 1977. Hydrologic And Ecologic Inventories of the Coastal Waters of West Hawai'i. Sea Grant College Program, Years 07-08. Technical Report No. 105 Sea Grant Cooperative Report UNIHI-SEAGRANT-CR-77-02. .